Stability Evaluation of High Frequency Eigen Modes for Active Magnetic Bearing Rotors

Hiroyuki Fujiwara
National Defense Academy, Yokosuka, Kanagawa, Japan, hiroyuki@cc.nda.ac.jp
Osami Matsushita
National Defense Academy, Yokosuka, Kanagawa, Japan, osami@cc.nda.ac.jp
Hiroki Okubo
National Defense Academy, Yokosuka, Kanagawa, Japan, ookubo@cc.nda.ac.jp

ABSTRACT

The servo feedback system of the active magnetic bearing (AMB) is commonly regulated by the PID control law. This law results in a very simple design. However it still contains several problems for the tuning of the control unit. In order to compensate for the insufficiency of the PID controller, a notch filter and a zero−pole canceling filter(z−p filter) are successfully introduced for tuning and stabilizing the high frequency vibration in our simulation and experiment. The stability margin of high frequency modes is increased by using these filters. For the stability evaluation, a new Nyquist plot on the log scale chart is introduced in this paper. The Nyquist plot provides the analysis of the global behavior of the locus of all eigen modes. The case study of the stability margin is presented concerning two rotors of the "long" and "flat" types, and the effective usage is demonstrated with respect to the new Nyquist plot.

1. INTRODUCTION

Active magnetic bearings(AMB) support a rotor without mechanical contact. The bearing force levitating the rotor is generated by electro−magnets, so that the AMB's force is controlled by a servo feedback control law. e.g., the PID control. More specifically this AMB force is controlled by the transfer function of the control loop from the sensor to the magnetic force.

The stablity of the AMB control system is evaluated by two parts; damping ratio of critical speeds within the operational speed range and stability margin of high frequency eigen modes over the operational speed range. The former is called Q−value evaluation which is already established by ISO10814. The latter is called high frequency mode instability which is discussed in this paper. The stability margin of the usual control theory is well studied as the gain and phase margin, but it is applicable only to simple rotors having low natural frequencies. Our investigation is to evaluate the stability margin of high frequency bending modes, called spill over instability.

This spill over instability is mainly caused by the phase lag of the controllers. The controllers phase lag is equivalent to the negative damping of mechanical systems. For the evaluation of this stability margin, we have to estimate the balance between the material positive damping of the rotor and the controller negative damping. One of the means to measure the stability margin is to directly increase the total gain of the controller. Another means is to make the comparison of both Q−factors between the open and closed loop responses. The Nyquist plot and the sensitivity function also provide good information on the stability margin.

We provide experimental data for our two test rotors; a flexible long rotor and a flat rotor like as a flywheel. In our levitation tests, we experienced the unstable vibrations corresponding to the high frequency eigen modes due to the flexibility of the long shaft and the thin flywheel disc. These unstable vibrations cannot be completely eliminated.

The reduced models of these rotor systems, equipped with AMBs, are first introduced for our numerical simulation. A typical example of the controller transfer function is prepared for the simulation. The transfer function of the global system, which combines the rotor model and the PID controller is examined in order to evaluate the stability margin. The stability margin is evaluated by several methods mentioned above.

In order to compensate for this insufficiency of the PID

controller, a notch filter and a zero−pole canceling filter(z−p filter) are successfully introduced for tuning and stabilizing the high frequency vibration in our simulation and experiment. For the stability evaluation, a new Nyquist plot on the log scale chart is introduced. This paper refers to it as the *"dB" Nyquist Plot*. The Nyquist plot is usually described in the linear chart, so that the overview of the plot locus will be easily outside the measurement range. However, the usage of this *"dB" Nyquist Plot* provides the analysis of the global behavior of the locus of all eigen modes. According to this new "*dB" Nyquist Plot*, we can retune the stability of the "long" and "flat" rotors prepared in our test. The usefulness of the stability evaluation method is proved by the tests with and without the z−p filter.

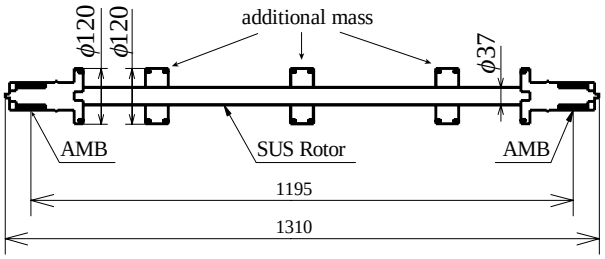

FIGURE 1: Structure of Rotor Model

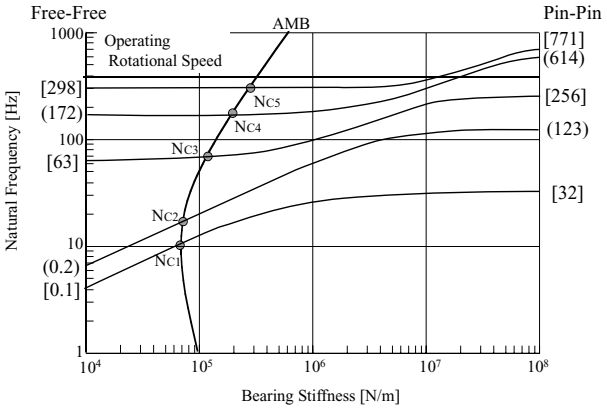

FIGURE 2 : Critical Speed Map of "Long" Rotor

2. "LONG " ROTOR AND "FLAT" ROTOR

2.1 Description of the Flexible "Long" Rotor

Figure 1 shows the structure of the rotor model. The rotor has a shaft diameter of ϕ37, a total length of 1310 mm and a total mass of 29.8kg. The shaft, connected by 2 AMB journals at both ends, has 3 discs placed between the bearing span. The AMBs are arranged on both sides with a bearing span of 1195 mm.[1]

In the rotational speed range, with a rated revolution of 350 rps, 5 resonant modes exist as shown in the critical speed map of Fig. 2. The horizontal axis is the stiffness of the AMB and the vertical axis is the natural frequency. Since the stiffness is drawn on the map, intersections indicate critical resonant speeds. As a resonant mode, it is a flexible rotor with the rigid modes of primary and secondary frequency(15Hz, 30Hz), and bending modes of first, second and third orders (65Hz, 175Hz, 175Hz).

Modeling of the "Long" Rotor: The equation of motion of the rotors and bearings, excluding the material damping term, can be expressed by the following formula:

$$[\mathbf{M}]\ddot{\mathbf{X}} + [\mathbf{K}]\mathbf{X} = \mathbf{Q}_{AMB} + \mathbf{U}\Omega^2 \qquad (1)$$

where **X** is a rotor radial complex displacement vector, **M** is a mass matrix, **K** is a shaft stiffness matrix, $\mathbf{Q}_{AMB}$ is a controlling force, **U** is a vector showing unbalance distribution of each point and Ω is a revolution speed. The equations of motion of the flexible rotor are formulated by the component mode synthesis.[3][4]

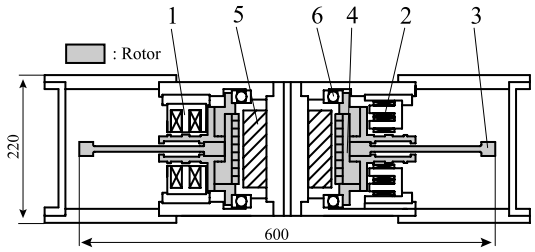

1:Axial AMB 2:Radial AMB 3:Flywheel Disk
4:Motor-Rotor 5:Motor-Stator 6:Auxiliary Bearing

FIGURE 3: Schematic of "Flat" Rotor

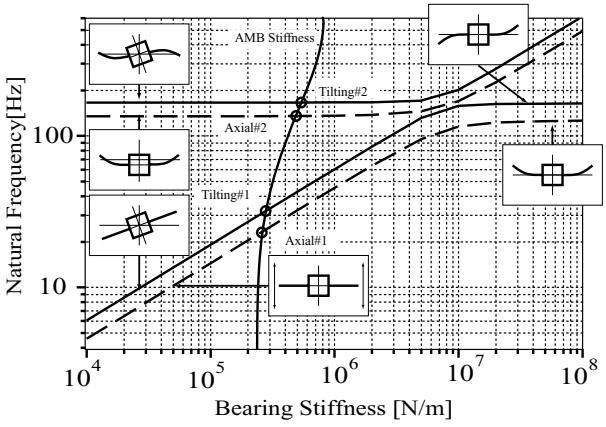

FIGURE 4:Critical Map of the "Flat" Rotor(Standstill)

2.2 Description of the "Flat" Rotor

A schematic of the "flat" test rotor, which looks like a flywheel, is shown in Fig 3.[2] The main characteristics of the "flat" rotor is as follows:

Flywheel diameter : 0.6m

Rotor mass : 36kg
Polar moment of inertia: 0.69kgm^2
Max. rotational speed : 200rps

The critical speed map of this rotor system is shown in Figure 4. When the stiffness of the AMB is set to approximately 3*10^5 [N/m], the natural frequencies of the rigid modes are 23Hz(Axial) and 30Hz(Tilting), and the bending modes are 137Hz(Axial) and 170Hz(Tilting).

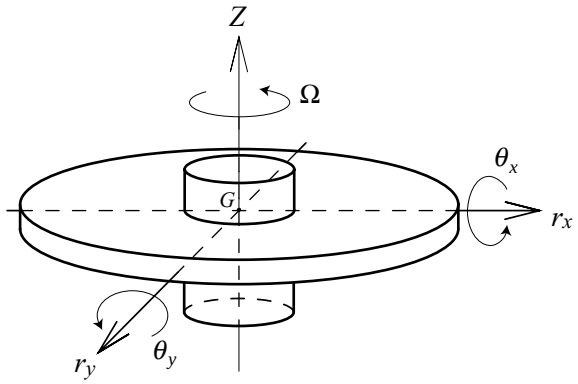

FIGURE 5: Rotor Coordinate System

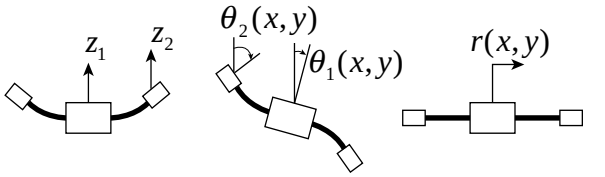

(1) axial (2DOF) (2) tilting (4DOF) (3) radial (2DOF)
FIGURE 6 : Flat Rotor Displacement Modes

Modeling of the "Flat" Rotor for Simulation: Figure 5 shows the structure of the "flat" rotor model and the coordinate system. The center part of the shaft is described by 5 DOF (r_x, r_y, θ_{1x}, θ_{1y}, z_1). Since the flexibility of the disc is considered, the disc mass is divided into two parts, i.e., inner and outer parts. As shown in (1) of Fig. 6, the axial motions are defined by z_1 of inner shaft motion and z_2 of the outer part of the disc. The vibration z_2 is one nodal−circular of the disc. As shown in (2) of Fig. 6, the declination motions are noted by θ_1 of the inner shaft motion and θ_2 of the outer plate. The vibration of θ_2 is the eigen mode of one nodal diameter of the disc. Considering the freedom of the inner shaft and the outer part of the disc, the corresponding equation of the motion is expressed as follows:

Axial: $$[\mathbf{M}]\ddot{\mathbf{Z}} + [\mathbf{K}_a]\mathbf{Z} = -\mathbf{Q}_{AMBa} \quad (2a)$$

Tilting: $$[\mathbf{I}_d]\ddot{\theta} - i\Omega[\mathbf{I}_p]\dot{\theta} + [\mathbf{K}_\theta]\theta = -l\mathbf{Q}_{AMBa} \quad (2b)$$

Radial: $$[\mathbf{M}]\ddot{\mathbf{r}} + [\mathbf{K}]\mathbf{r} = -\mathbf{Q}_{AMBr} \quad (2c)$$

Where:
Z : $[z_1,z_2]^t$,the displacement in the axial direction
M : the rotor mass matrix
K_a : the stiffness matrix in the axial direction
Q_{AMBa} : the axial AMB control force matrix
I_d : the tilting transverse moment of inertia
θ : $[\theta_1,\theta_2]^t$, the complex declination angle $(\theta_x+i\theta_y)$
I_p : the polar moment of inertia of the rotor
K_θ : the tilting stiffness matrix
l : the length from geometrical center of the rotor to geometrical center of axial AMB
r : the complex displacement(r_x+ir_y)
K : the stiffness matrix
Q_{AMBr} : the radial AMB control force
An equivalent mass for (z_2, θ_{2x}, θ_{2y},) modes is estimated by the modal synthesis method.

3. OPEN AND CLOSED LOOP TRANSFER FUNCTION

Figure 7 shows the feedback system of the rotor and the controller. The open loop transfer function of the global system G_o is generally as follows:

$$G_o = G_p G_r \quad (3)$$

where G_p is the transfer function of the rotor system without the controller and G_r is the transfer function of the controller. In this paper, the control system of G_r is mainly prepared by the PID control. The closed loop transfer function G_c is shown as follows:

$$G_c = \frac{G_o}{1+G_o} \quad (4)$$

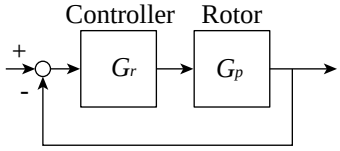

FIGURE 7: Feedback System of the Rotor and the Controller

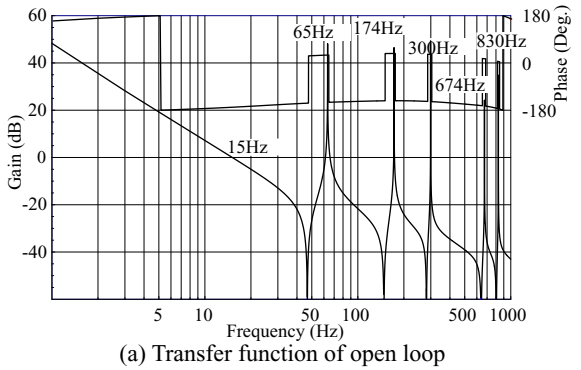

(a) Transfer function of open loop

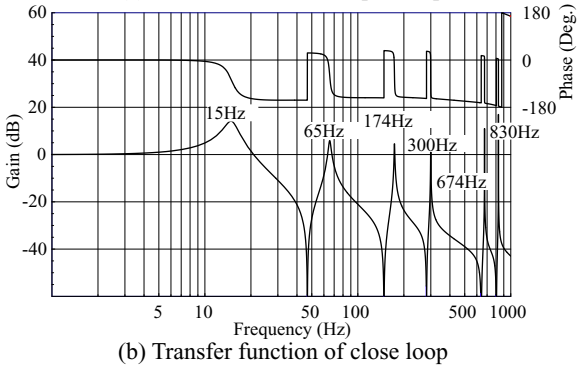

(b) Transfer function of close loop

FIGURE8: Open and Closed Loop Transfer Function of the "Long" Rotor

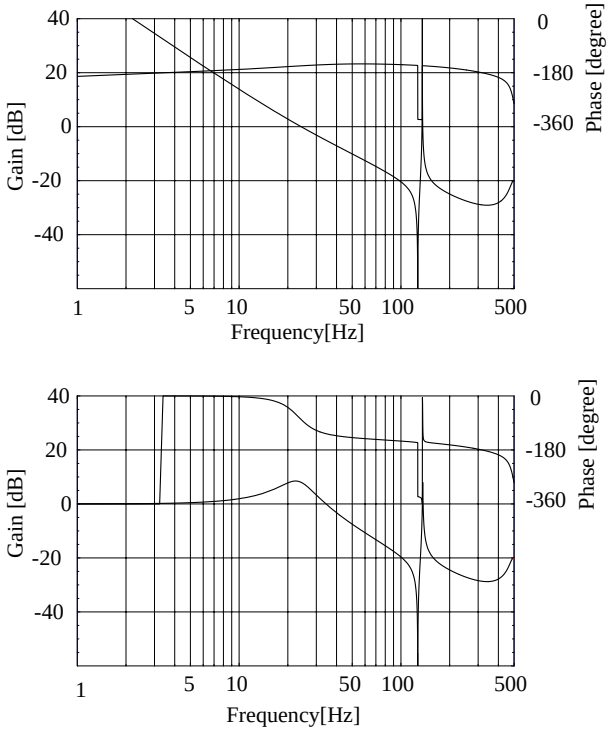

FIGURE 9: Open and Closed Loop Transfer Function of "Flat" Rotor in Axial Direction

3.1 The "Long" Rotor

The characteristics of the open loop and closed loop are examined for the "long" rotor model, considering a total of five bending modes as shown in Fig. 5. In this "long" rotor model, there are rigid modes, a bending mode of the first order (65 Hz), a bending mode of the second order (174 Hz) and a bending mode of the third order (300 Hz) in the range of the rated revolution of 350 rps. Further more, there are bending modes with higher frequencies over the rated speed. These higher eigen modes are induced to be unstable.

3.2 The "Flat" Rotor

In Figure 9, the characteristics of the open loop and closed loop are examined with respect to the "flat" rotor model of the axial direction. In this "flat" rotor model, there are a rigid mode and a bending mode of the first order respectively, 23[Hz] and 137[Hz].

4. IMPROVEMENT OF HIGHER FREQUENCY RESONANT VIBRATION

4.1 Notch Filter and z−p Cancellation Filter

The prepared PID controller is then unable to eliminate the instability in the high frequency domain. In order to compensate for this insufficiency of the PID controller, a notch filter and a zero−pole canceling filter(z−p filter) are successfully introduced for tuning and stabilizing the high frequency vibration in our simulation and experiment. We add a notch filter and zero−pole canceling filter, as shown in the following formulas:

notch filter
$$G_E = \frac{s^2 + \omega_z^2}{s^2 + 2\zeta_e \omega_z s + \omega_z^2} \qquad (5)$$

z−p filter
$$G_{ZP} = \frac{s^2 + \omega_z^2}{s^2 + 2\zeta_p \omega_p s + \omega_p^2} \frac{\omega_p^2}{\omega_z^2} \qquad (6)$$

where ζ_e and ζ_p are damping. ω_z, and ω_p are frequencies.

4.2 Effect of the Filters

Figure10(a) shows the typical open loop transfer function of a flexible rotor system, which includes an unstable vibration near an eigen frequency ω_{f2}. Figure10 (b) is the corresponding Nyquist plot of the system. The system is unstable, because the locus draws the overlaping critical point (−1,0).

Figure10(c) shows the transfer function of the notch filter. The addition of the notch filter can generate a stabilization of the rotor system. By using the filters, we must coinside the ω_z with ω_f. In this manner,

Figure10(d) shows the transfer function of z−p the filter. The addition of the z−p filter can generate a stabilization of the rotor system. By using the filters, we must coinside in ω_z with ω_f. Figure 10(e)(f) show the Nyquist plots of the rotor systems, combined with each filter. The results show that stability margin of both systems are increased.

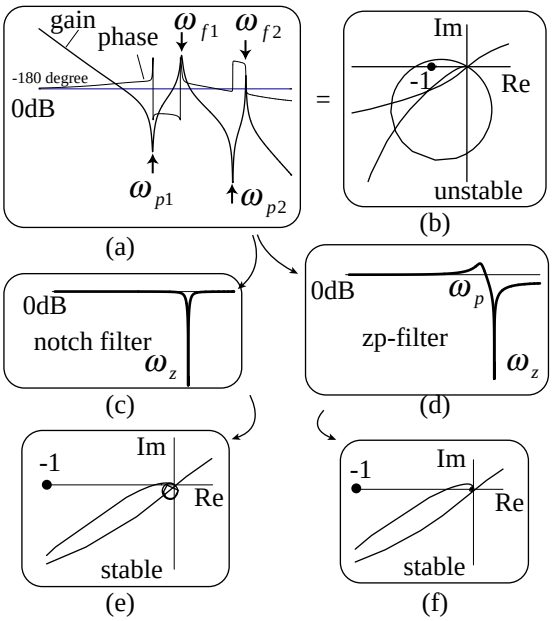

FIGURE 10: Effects of the Notch Filter and the z−p Filter

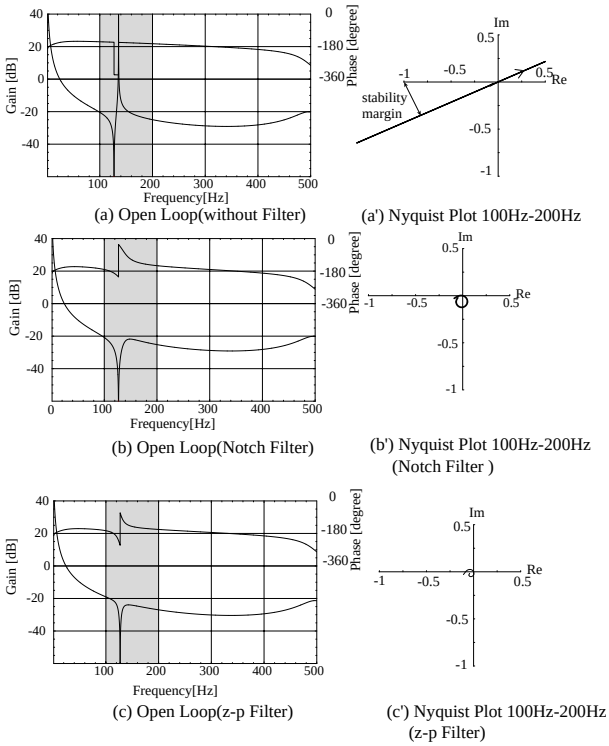

FIGURE 11: Stability of the "Flat" Rotor System

4.3 Simulation of the "Flat" Rotor Model

Figure 11 shows the effectiveness of adding the notch filter or z−p filter:
(a) is the open loop of the plant(rotor)
(b) is the open loop of the plant plus the notch filter
(c) is the open loop of the plant plus the z−p filter
On the left side, we place Bode diagrams of these (a),(b),(c) and on the right side, the corresponding Nyquist diagram in the range of [110−200]Hz.
Since the locus of the open loop including these filters in the Nyquist plot, are modified to be very far from the critical point (−1,0), the system stability is greatly improved.

5. THE NEW NYQUIST PLOT

For the stability evaluation, a new Nyquist plot on the log scale chart is introduced. This paper refers to it as the *"dB" Nyquist plot*.

$$v = \left(20\log\left|G(j\omega)\right|\right)e^{j\theta(\omega)} \qquad (7)$$

where $G(j\omega)$ is a transfer function and θ is a phase angle. *"dB" Nyquist plot* is the plot locus of **v** on the complex plane. The Nyquist plot is usually described in the linear chart, so that the overview of the plot locus will be easily outside the measurement range. However, the usage of this *"dB" Nyquist plot* provides the analysis of the global behavior of the locus of all eigen modes. The stability margin is given by the distance from the critical point which is (1,0) on the Nyquist plot. It is noted that the *"dB" Nyquist plot* is equal to an actual distance on the linear Nyquist chart. Figure 12 shows *the "dB" Nyquist plot* converted from the Nyquist plot of the simulation data in Fig. 11(c'). As shown in these figures, it is easy to analyze the global behavior of the system.

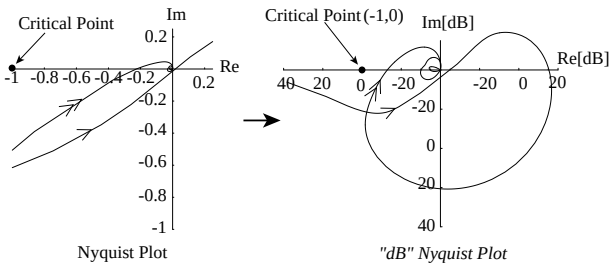

FIGURE 12: Characteristic of *"dB" Nyquist Plot*

6. EXPERIMENTAL RESULT

According to this new *"dB" Nyquist plot*, we can retune the stability of the "long" rotor and the "flat" rotor in

our tests. The usefulness of the stability evaluation method is proved by the tests with and without the z−p filter.

6.1 the "Long" Rotor

The test data obtained from the "long" rotor is displayed in Fig.13. An example of the open loop bode plot is shown in Fig.13 (1). It is measured by a usual FFT analyzer. In this open loop gain curve, many peaks of bending mode eigen frequencies appear. This bode plot data is rearranged, and it is redrawn in the *"dB" Nyquist plot* Fig.13 (2). The detail plot around 645Hz, selecting a part of (2), is shown in Fig. 13(3). In the case of the additional z−p filter, the Bode plot is measured and the corresponding *"dB" Nyquist plot* is rearranged, as shown in Fig. 13(4). As the result of the zero−pole filter(ω_p=585[Hz],ω_z=642[Hz]), the distance margin is increased.

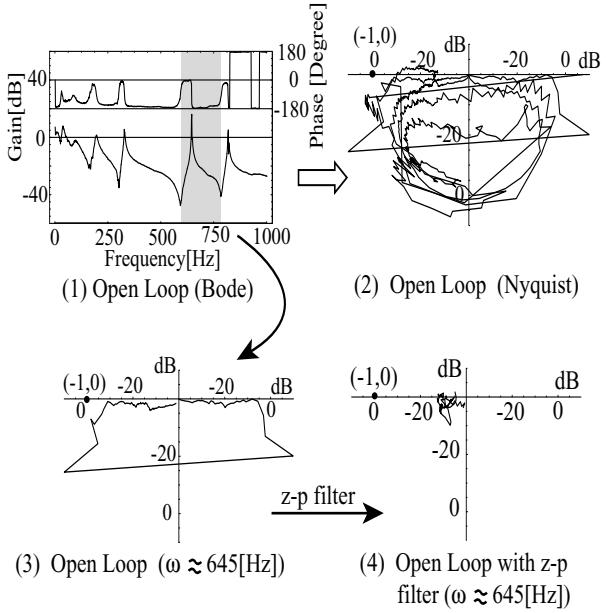

FIGURE 13: *"dB" Nyquist Plot* of the "Long" Rotor

6.2 the "Flat" Rotor

The data obtained from the "flat" rotor is displayed in Fig. 14. An example of the open loop Bode plot is shown in Fig. 14 (1). This Bode plot data is rearranged , and it is redrawn in the *"dB" Nyquist plot* Fig. 14 (2). The detail plot around 120 [Hz], selecting a part of (2), is shown in Fig. 14 (3). In the case of the additional z−p filter, the Bode plot is measured and the corresponding *"dB" Nyquist plot* is rearranged, as shown in Fig. 14 (4). As the result of the z−p filter (ω_p=118[Hz], ω_z=104[Hz]), the distance margin is increased.

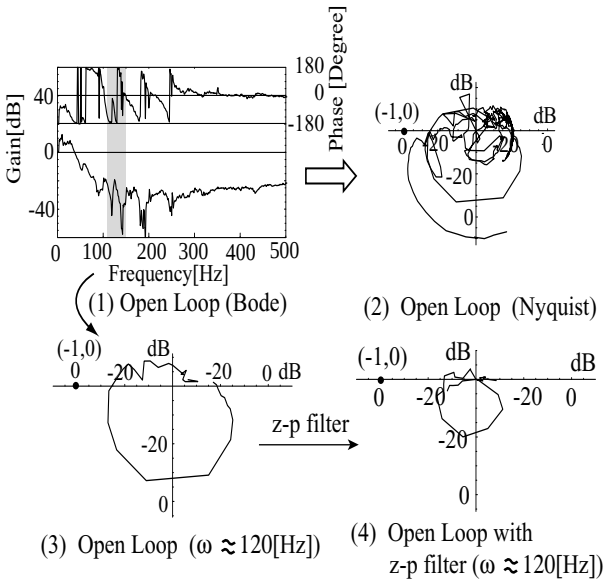

FIGURE 14: *"dB" Nyquist Plot* of a Flat Rotor

7. CONCLUSION

In this paper, a notch filter and a zero−pole canceling filter(z−p filter) are introduced for tuning the stabilization of the high frequency vibration in our simulation and experiment. The stability margin of the high frequency modes are increased by using these filters. For the stability evaluation, the *"dB" Nyquist plot* on the log scale chart is introduced. The Nyquist plot provides good information for the analysis of the global behavior of the locus of all eigen modes.

8. REFERRENCES

[1] Makoto Ito, et. al, Unbalance Vibration Control For High Order Bending Critical Speeds of Flexible Rotor Supported by Active Magnetic Bearing, Proceeding of 8th International Symposium on Transport Phenomena and Dynamics of Rotating Machinery, pp.923−928,2000

[2] Keiji Katsuno, et. al, Vibration Control on Active Magnetic Bearing Equipped Flywheel Rotor, 5th InterNational Symposium on Magnetic Suspension Technology, 1999

[3] Matsushita, O. et al., Modeling; Free from Boundary Condition, Trans. Jpn. Soc. Prec. Eng., Vol.51, No.588, C, pp.44−48., 1988, (In Japanese)

[4] Takahashi, N. et al., Modeling for Flexible Mechanical Vibration Systems, proceeding of 18th SICE Symposium on Control Theory, pp.217−222. 1988 (In Japanese)